Thrust faults along the dichotomy boundary in the eastern hemisphere of Mars

Thomas R. Watters

Center for Earth and Planetary Studies, National Air and Space Museum, Smithsonian Institution, Washington, D.C., USA

Received 3 May 2002; revised 8 November 2002; accepted 26 February 2003; published 14 June 2003.

[1] Mars Orbiter Laser Altimetry (MOLA) data have been used to characterize lobate scarps along the dichotomy boundary in the eastern hemisphere of Mars. These structures are the surface expression of thrust faulting of the southern highlands. Displacement on the thrust faults is generally less than 1 km except in the case of the Amenthes Rupes thrust fault, where the maximum displacement is on the order of 3 km. The ratio of maximum displacement to fault length γ of the population of thrust faults is $\sim 6.2 \times 10^{-3}$ ($n = 26$), consistent with previous estimates for Martian thrust faults based on photoclinometrically derived topography, and other planetary thrust fault populations. Thrust faulting is roughly coincident with Late Noachian to Early Hesperian fracturing and normal faulting along the dichotomy boundary. This suggests that the formation of the present-day dichotomy boundary involved compressional and extensional deformation. The long-wavelength topography suggests that the dichotomy boundary in the eastern hemisphere may have been formed by flexure of the southern highlands lithosphere. Lithospheric flexure alone cannot account for the thrust faulting of the highlands along the dichotomy boundary. A combination of stresses due to bending, erosion, and global contraction may have formed the lobate scarp thrust faults. *INDEX TERMS:* 5475 Planetology: Solid Surface Planets: Tectonics (8149); 5415 Planetology: Solid Surface Planets: Erosion and weathering; 5430 Planetology: Solid Surface Planets: Interiors (8147); 6207 Planetology: Solar System Objects: Comparative planetology; *KEYWORDS:* Thrust faults, dichotomy boundary, lobate scarps, Mars, lithospheric flexure

Citation: Watters, T. R., Thrust faults along the dichotomy boundary in the eastern hemisphere of Mars, *J. Geophys. Res.*, *108*(E6), 5054, doi:10.1029/2002JE001934, 2003.

1. Introduction

[2] The surface of Mars reflects tectonism on a regional and hemispheric scale [*Wise et al.*, 1979; *Watters*, 1993]. Both extension and compression have played major roles in the tectonic evolution of the planet. Mars Global Surveyor (MGS) has returned a wealth of new data that has dramatically changed our view of the planet [*Zuber*, 2001]. The topography of Martian tectonic features can now be characterized with great accuracy using Mars Orbiter Laser Altimetry (MOLA) data [*Smith et al.*, 1999, 2001; *Zuber et al.*, 2000]. Global topography and gravity data suggest that the Tharsis dominated western hemisphere influenced topography and tectonics on a global scale [*Phillips et al.*, 2001]. However, there is evidence that tectonic features in the eastern hemisphere of Mars were influence by another major feature, the dichotomy boundary [*Watters*, 1993, 2003; *Watters and Robinson*, 1999].

[3] Lobate scarps in the highlands of Amenthes-northern Terra Cimmeria and northern Arabia Terra are examined using MOLA data. These structures and fractures and normal faults are the dominant tectonic features along the dichotomy boundary. Lobate scarps are interpreted to be the surface expression of thrust faulting of highland materials near the dichotomy boundary [*Watters*, 1993; *Watters and Robinson*, 1999; *Watters et al.*, 2000; *Schultz and Watters*, 2001]. Fractures and normal faults occur along the dichotomy boundary and in the adjacent lowlands [*McGill and Dimitriou*, 1990]. The topography of lobate scarps is determined, and the displacement-length relationships of the underlying thrust faults are estimated. The relationship between the dichotomy boundary and the lobate scarps is examined. Finally, implications for the origin of the stresses that formed the lobate scarp thrust faults are discussed.

2. Lobate Scarps

[4] Lobate scarps are landforms found on Mercury, the Moon, and Mars [*Howard and Muehlberger*, 1973; *Strom et al.*, 1975; *Lucchitta*, 1976; *Cordell and Strom*, 1977; *Binder*, 1982; *Binder and Gunga*, 1985; *Melosh and McKinnon*, 1988; *Watters*, 1993; *Watters and Robinson*, 1999; *Watters et al.*, 1998, 2000, 2001]. The fact that these structures often deform impact craters has led to the unanimous interpretation that lobate scarps are the surface manifestation of thrust faulting. A kinematic model applied to lobate scarps involves a planar thrust fault that propagates upward even-

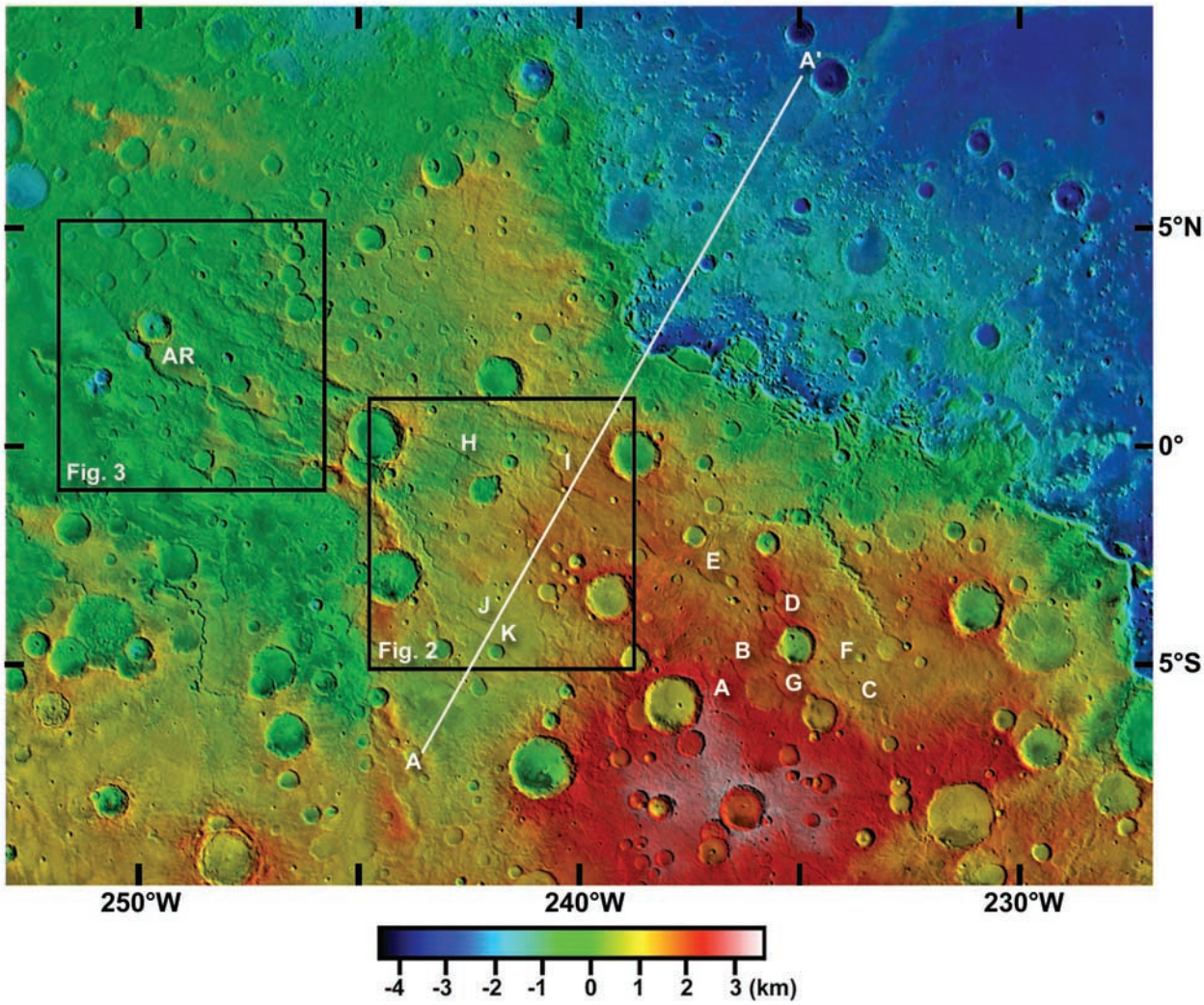

Figure 1. Color-coded MOLA digital elevation model of Amenthes-northern Terra Cimmeria overlaid on a Viking Orbiter image mosaic. The NW-SE trending scarp marks the dichotomy boundary between the southern heavily cratered highlands and the northern lowlands. The black boxes indicate the locations of Figures 2 and 3. The white line indicates the location of the topographic profile shown in Figure 8. The white letters show the location of the lobate scarps described in Table 1. The digital elevation data are from the MOLA gridded 1/32° per pixel resolution model.

tually breaking the surface [*Watters and Robinson*, 1999]. Elastic dislocation modeling of the faults underlying Amenthes Rupes on Mars and Discovery Rupes on Mercury, constrained by topography, supports the interpretation that they were formed by thrust faults with planar geometries [*Schultz and Watters*, 2001; *Watters and Schultz*, 2002; *Watters et al.*, 2002].

2.1. Amenthes–Northern Terra Cimmeria

[5] The lobate scarps in the heavily cratered highlands of Amenthes-northern Terra Cimmeria have orientations that parallel the steep scarp that marks the dichotomy boundary (Figure 1). The topography of lobate scarps in Amenthes-northern Terra Cimmeria has been determined using MOLA data. The Mars Orbiter Laser Altimeter (MOLA) has provided global high-resolution topographic data for Mars [*Smith et al.*, 1998, 1999, 2001; *Zuber et al.*, 1992, 2000]. These data have a maximum vertical resolution of about 30 cm and along-track spatial resolution of 300 to 400 m [*Smith et al.*, 1998]. The relief and morphology of lobate scarps were examined by generating digital elevation models (DEMs) from MOLA orbital profiles. The data were gridded at a spatial resolution of 300 m/pixel and then interpolated using kriging (Figure 2). Crossover statistics were collected for each MOLA orbital profile in the DEM area [see *Neumann et al.*, 2001]. These data are analyzed to determine if a given orbital profile is offset relative to others in the DEM area. If an orbital profile is significantly offset, it was not included in the DEM. Profiles across the lobate scarps were then generated in several locations (usually 3 to 4) to determine the maximum relief. Measurements of maximum relief on moderate-scale lobate scarps using the MOLA-based DEMs range from 158 to 364 m with a mean of 241 m (n = 11) (Table 1). These measurements are in

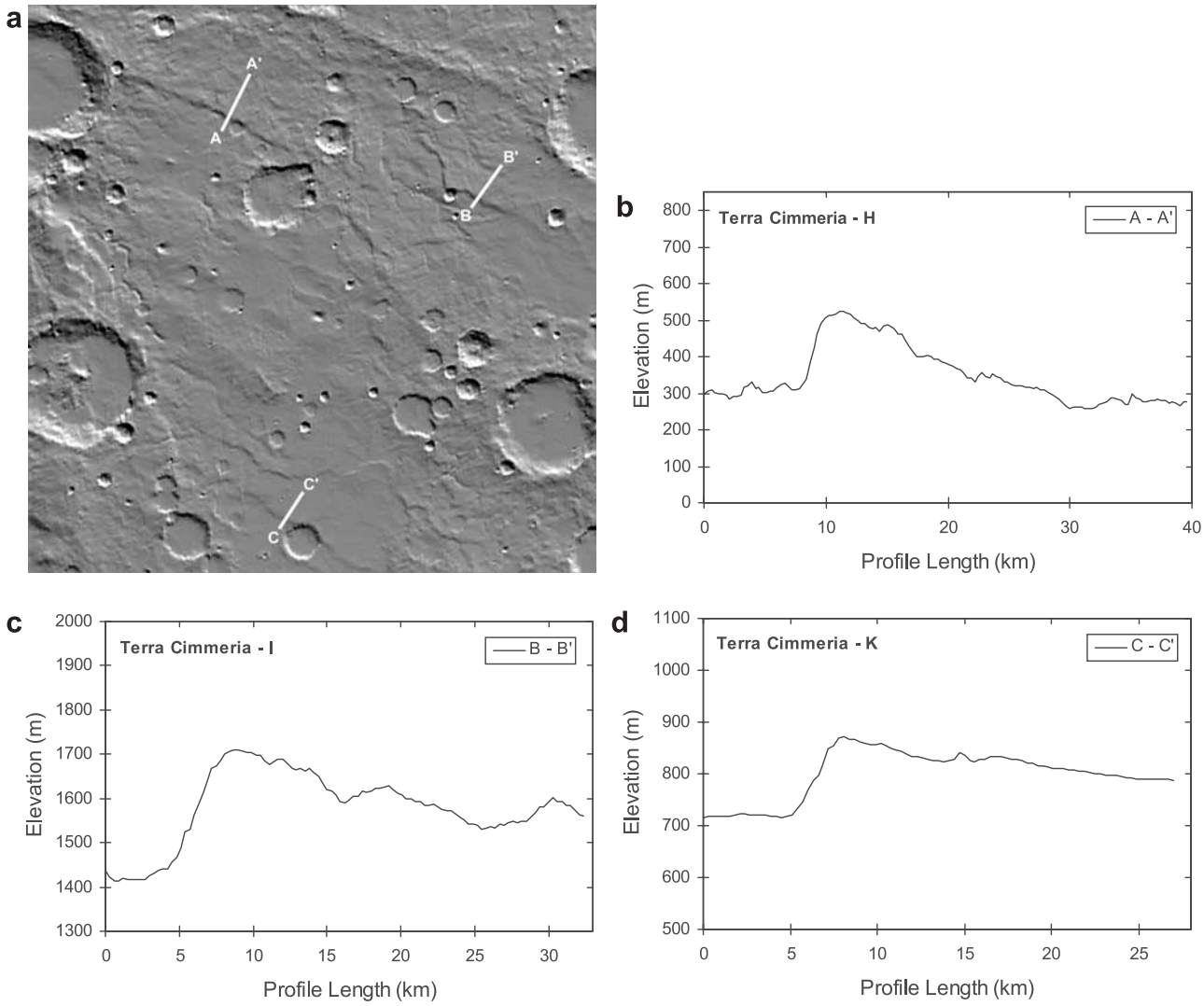

Figure 2. (a) Shaded relief image of an area in northern Terra Cimmeria derived from MOLA data gridded at 300 m/pixel. (b) Profile across a lobate scarp H (vertical exaggeration is ~30:1). (c) Profile across a lobate scarp I (vertical exaggeration is ~30:1). (d) Profile across a lobate scarp K (vertical exaggeration is ~30:1). The locations of the profiles are shown in Figure 2a (see Table 1).

excellent agreement with the range determined with photoclinometric measurements (112 ± 9 m to 315 ± 24 m) [*Watters and Robinson*, 1999].

[6] The most prominent lobate scarp along the dichotomy boundary in the eastern hemisphere is Amenthes Rupes (Figure 3). It has greater relief and length than moderate-scale scarps found in northern Terra Cimmeria [*Watters and Robinson*, 1999]. Amenthes Rupes is ~380 km in length, comparable in scale to Discovery Rupes, the largest known lobate scarp on Mercury [*Watters et al.*, 1998, 2000, 2001]. The maximum relief of Amenthes Rupes determined from a MOLA-based DEM is 1228 m (Figure 3). This is in excellent agreement with measurements made using photoclinometry (1225 ± 92 m) [*Watters and Robinson*, 1999].

[7] Topographic profiles across Amenthes Rupes and the other lobate scarps clearly reflect basic morphologic elements. They are asymmetric landforms with relatively steep sloping scarp faces and gently sloping back scarps (Figures 2 and 3). The profiles also indicate that the vergent side of

Table 1. Dimensions of Lobate Scarps in Amenthes–Northern Terra Cimmeria[a]

Index	Latitude	Longitude	Maximum Relief, m	Length, km	D $\theta = 25°$, m	D/L
A	6.1°S	237.0°W	241	94.6	570.3	0.006
B	5.1°S	236.6°W	179	39.5	423.3	0.0107
C	5.8°S	234.0°W	175	89.4	414.1	0.0046
D	3.9°S	235.6°W	281	64.4	664.9	0.0103
E	2.7°S	237.8°W	364	137.1	861.3	0.0063
F	4.8°S	234.4°W	245	39.7	579.7	0.0146
G	5.5°S	235.6°W	226	44.0	534.8	0.0122
H	0.1°S	243.0°W	214	111.9	506.4	0.0045
I	0.9°S	240.6°W	343	76.9	811.6	0.0106
J	3.9°S	242.5°W	225	93.2	532.4	0.0057
K	4.5°S	242.2°W	158	81.0	373.9	0.0046
AR	1.5°N	249.5°W	1228	381	2905.7	0.0076

[a]The locations of the lobate scarps are shown in Figure 1.

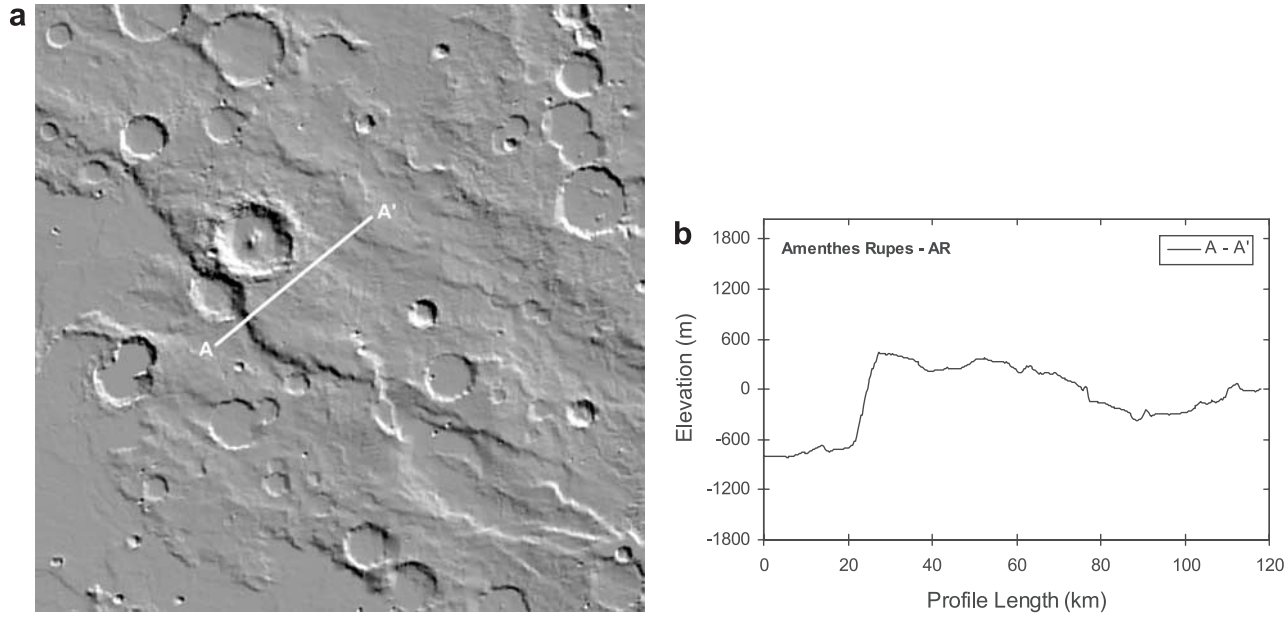

Figure 3. (a) Shaded relief image of Amenthes Rupes derived from MOLA data gridded at 300 m/pixel. (b) Profile across Amenthes Rupes AR (see Table 1). The location is shown in Figure 3a (vertical exaggeration is ~20:1.)

the structures face away from the dichotomy boundary (Figures 1–3). This suggests that the thrust faults underlying all the lobate scarps studied in Amenthes-northern Terra Cimmeria dip toward the dichotomy boundary.

2.2. Northern Arabia Terra

[8] Lobate scarps in northern Arabia Terra, like those in the Amenthes region, are oriented roughly parallel to the dichotomy boundary (Figure 4). Although these scarps occur in units mapped by *Greeley and Guest* [1987] as Noachian ridged plains (Nplr), the intercrater plains they deform are indistinguishable from the highlands of Amenthes and northern Terra Cimmeria mapped as Noachian plains (Npld). The most prominent lobate scarp in northern Arabia Terra is located less than 200 km from the dichotomy boundary. Informally named Ismenius Rupes, this large-scale lobate scarp has a maximum relief of about 500 m and is over 300 km in length (Figures 5a and 5b). The maximum relief of the moderate-scale lobate scarps measured range from ~127 to 457 m with a mean of 286 m (n = 12) (Table 2). Some of the lobate scarps in northern Arabia Terra appear more prominent than moderate-scale lobate scarps in northern Terra Cimmeria (Figures 4 and 5). This may reflect the greater average relief of the lobate scarps in northern Arabia Terra (see Table 2). In contrast to the lobate scarps in Amenthes-northern Terra Cimmeria, the vergent side of some of the lobate scarps in northern Arabia Terra (particularly those closest to the dichotomy) face toward the dichotomy boundary (Figures 4 and 5). This suggests that thrust faults dip both toward and away from the dichotomy boundary in northern Arabia Terra.

[9] Another lobate scarp in Arabia Terra marks the western rim of a previously unknown basin. This basin, identified using MOLA data, is about 450 km wide and up to 2 km deep [*Frey et al.*, 1999]. The lobate scarp is locally sinuous over its length but forms a linear segment of the rim of the basin. It is clear the lobate scarp postdates the formation of the basin and the subsequent emplacement of the intercrater plains. The thrust fault that formed the lobate scarp appears to have been influenced by the presence of the basin. This is reflected by the coincidence of the scarp face and the slopes of the basin rim, which are indistinguishable (Figure 6). The localization of lobate scarps by buried ancient impact basins is not unique to Mars. Recent studies of topography generated from Mariner 10 stereo pairs suggest that a number of prominent mercurian lobate scarps, including Discovery Rupes, may have been localized by an ancient buried basin [*Watters et al.*, 2001].

2.3. Displacement Length Relationships

[10] The maximum displacement D on a fault scales with the planimetric length of the fault L [*Walsh and Watterson*, 1988; *Cowie and Scholz*, 1992; *Cartwright et al.*, 1995]. This relationship also holds for planetary faults [*Schultz*, 1997, 1999; *Watters et al.*, 1998, 2000; *Watters and Robinson*, 1999]. D and L are related by $D = cL^n$, where c is a constant related to material properties and n is the power law exponent [*Walsh and Watterson*, 1988]. Studies of terrestrial faults in populations formed in uniform rock types, however, support a linear relationship $D = \gamma L$, where γ is a constant determined by rock type and tectonic setting (and n = 1) [see *Cowie and Scholz*, 1992; *Clark and Cox*, 1996]. The ratio of maximum displacement to fault length γ of terrestrial fault populations ranges between 10^0 and 10^{-3}. Scatter in the D-L data can arise from several sources including fault segmentation, uncertainties in fault dip and depth, interaction with other faults, and ambiguities in determining D along the fault [*Cartwright et al.*, 1995, *Dawers and Anders*, 1995; *Wojtal*, 1996; *Schultz*, 1999].

[11] The displacement necessary to restore the topography to a planar surface is given by $D = h/\sin\theta$ where h is the relief of the lobate scarp and θ is the dip of the fault plane

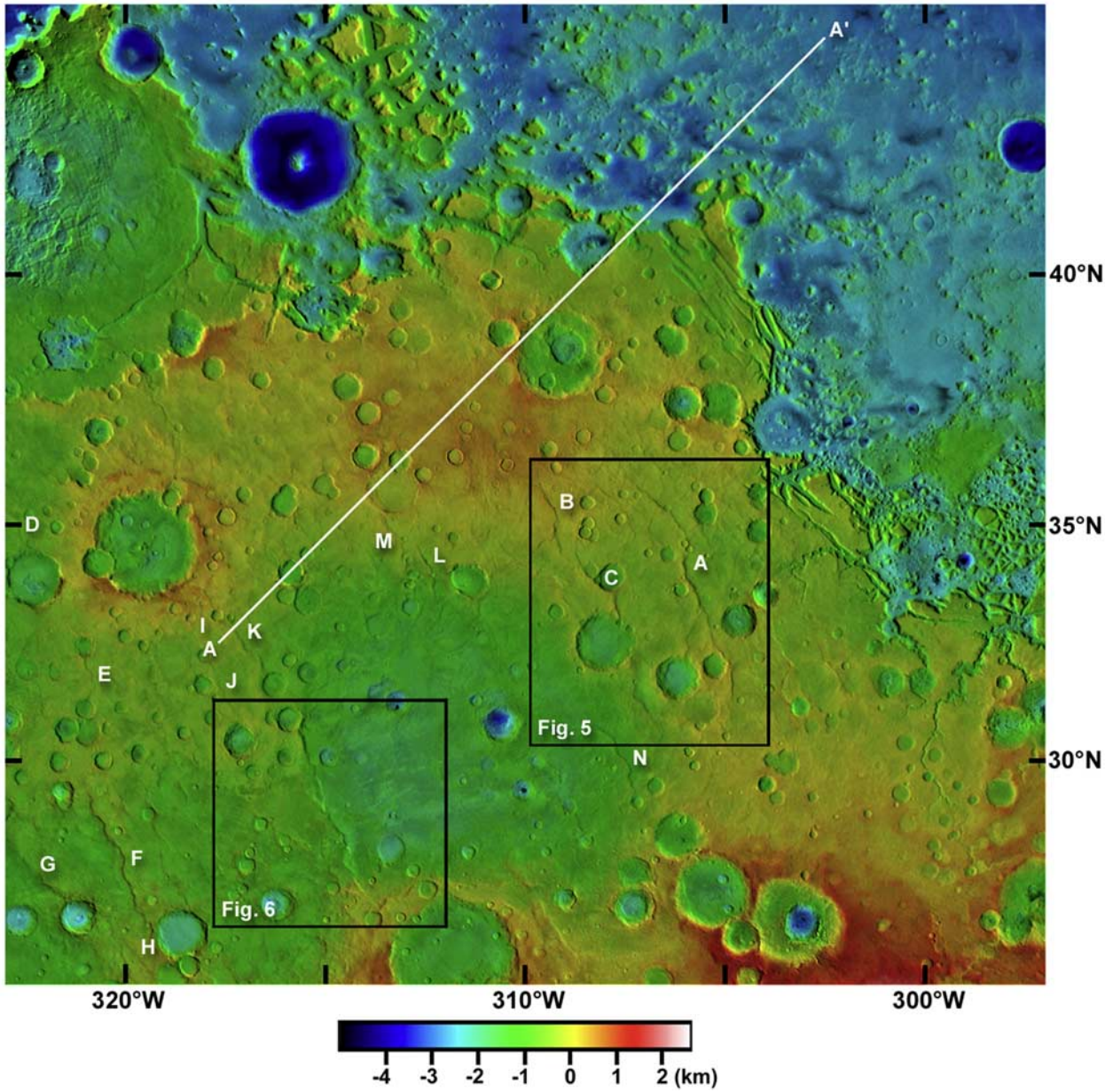

Figure 4. Color-coded MOLA digital elevation model of the northern Arabia Terra region overlaid on a Viking Orbiter image mosaic. The black boxes indicate the locations of Figures 5 and 6. The white line indicates the location of the topographic profile shown in Figure 9. The white letters indicate the location of the lobate scarps described in Table 2. The digital elevation data are from the MOLA gridded 1/32° per pixel resolution model.

[*Wojtal*, 1996; *Watters and Robinson*, 1999; *Watters et al.*, 2000]. Faulting will occur at the angle θ for which the differential horizontal stress necessary to initiate faulting is a minimum, given by $tan2\theta = 1/f_s$ where f_s, the coefficient of static friction, typically ranges from ~0.6 to 0.9 [*Byerlee*, 1978; *Jaeger and Cook*, 1979; *Turcotte and Schubert*, 1982]. This range in f_s corresponds to thrust faults with dips of about 24° to 30°, consistent with field observations of thrust faults that generally range from 20 to 35° [e.g., *Jaeger and Cook*, 1979; *Brewer et al.*, 1980; *Gries*, 1983; *Stone*, 1985]. Using measurements of the maximum relief of the lobate scarps from MOLA topography, displacements on the underlying thrust faults in Amenthes-northern Terra Cimmeria and northern Arabia Terra range from 0.3 to 1.2 km, assuming $\theta = 25°$, with an average of ~0.65 km ($n = 25$) (Tables 1 and 2). The maximum displacement on the Amenthes Rupes thrust fault is on the order of 2.90 km for $\theta = 25°$.

[12] Elastic dislocation modeling of the Amenthes Rupes and Discovery Rupes thrust faults support estimates of displacement and the assumed fault plane dips [*Schultz and Watters*, 2001; *Watters et al.*, 2002]. Fault parameters including geometry and depth of faulting were constrained by comparing the predicted structural relief with the surface topography. Best-fits of topographic profiles across

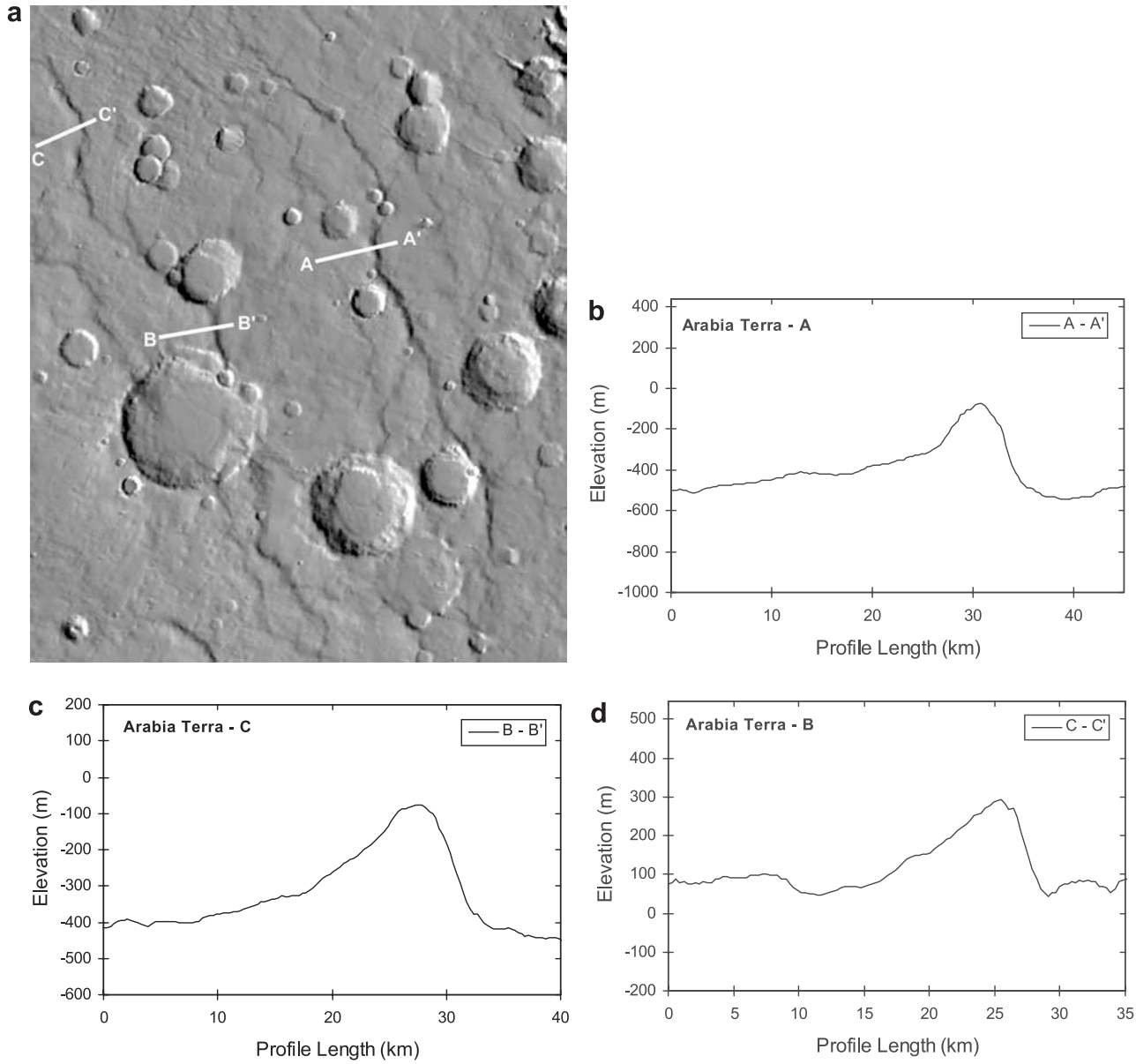

Figure 5. (a) Shaded relief image of an area in the northern Arabia Terra region derived from MOLA data gridded at 300 m/pixel. (b) Profile across a lobate scarp A (vertical exaggeration is ~20:1). (c) Profile across a lobate scarp C (vertical exaggeration is ~30:1). (d) Profile across a lobate scarp B (vertical exaggeration is ~30:1). The locations of the profiles are shown in Figure 5a (see Table 2).

Amenthes and Discovery Rupes are obtained for planar fault geometries with dips of 25° to 35°. The model displacements agree well with displacements estimated using the trigonometric relationship for kinematic reconstruction described above [*Schultz and Watters*, 2001; *Watters et al.*, 2002].

[13] Fault lengths were estimated by dividing the lobate scarps into sections with roughly uniform orientations and digitally measuring their lengths using a map-based tool. The lack of segmentation of lobate scarps and en echelon steps, as is often the case for Martian graben [e.g., *Schultz and Fori*, 1996] and wrinkle ridges [e.g., *Watters*, 1988], suggests that the thrust faults are continuous structures rather than a series of fault segments. An exception is Amenthes Rupes, where the eastern terminus of the struc-

Table 2. Dimensions of Lobate Scarps in Northern Arabia Terra[a]

Index	Latitude	Longitude	Maximum Relief, m	Length, km	D $\theta = 25°$, m	D/L
A	33.1°N	305.8°W	500	314.9	1183.1	0.0038
B	34.9°N	309.4°W	279	111.4	660.2	0.0059
C	33.2°N	308.0°W	432	99.8	1022.2	0.0102
D	34.7°N	322.8°W	136	67.9	321.8	0.0047
E	31.8°N	321.2°W	231	103.5	546.6	0.0053
F	27.3°N	320.2°W	457	197.3	1081.4	0.0055
G	27.0°N	322.2°W	438	62.4	1036.4	0.0166
H	25.1°N	319.6°W	262	131.3	619.9	0.0047
I	32.4°N	318.4°W	299	81.9	707.5	0.0086
J	31.2°N	317.8°W	127	67.0	300.5	0.0045
K	32.2°S	317.2°W	285	139.9	674.4	0.0048
L	33.8°S	312.6°W	258	76.3	610.5	0.008
M	34.1°S	314.0°W	171	70.0	404.6	0.0058
N	29.8°S	307.8°W	345	100.3	816.3	0.0081

[a]The locations of the lobate scarps are shown in Figure 4.

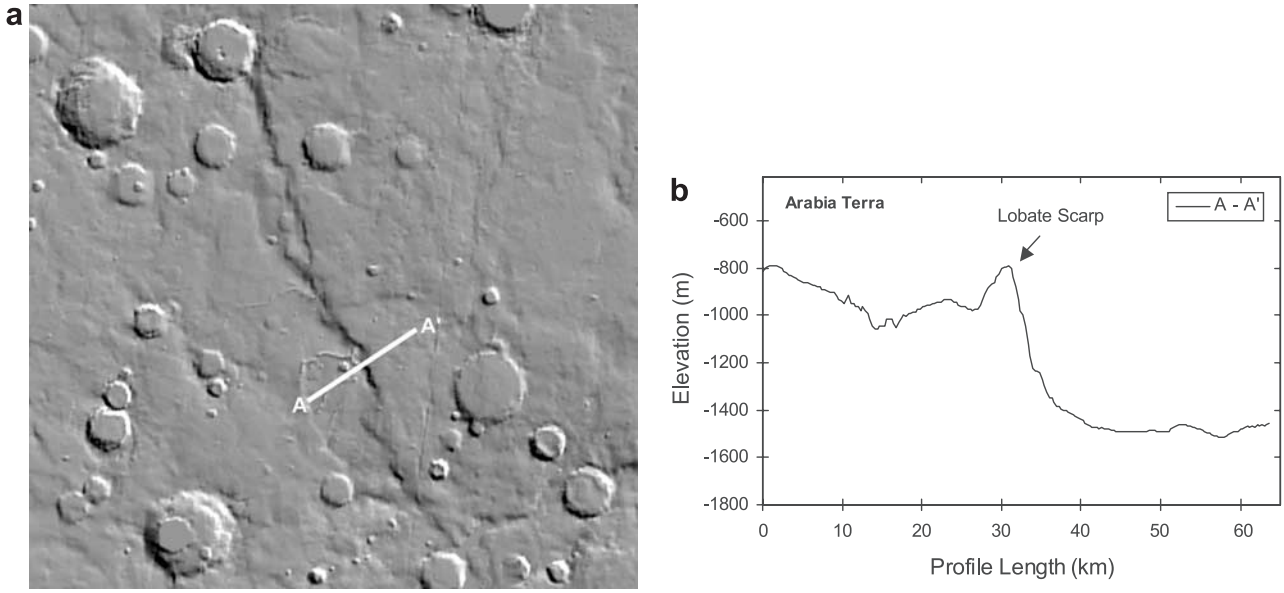

Figure 6. (a) Shaded relief image of a lobate scarp on the rim of an ancient buried basin in northern Arabia Terra. The image is derived from MOLA data gridded at 300 m/pixel. (b) Profile across the lobate scarp and part of an ancient buried impact basin. The location is shown in Figure 6a (vertical exaggeration is ~30:1).

ture is comprised of a complex series of thrust faults. Two strongly curvilinear thrust faults crosscut the more linear Amenthes Rupes thrust fault (Figure 3a). These faults have straight segments that parallel the NW-SE trend of Amenthes Rupes. The length of the Amenthes Rupes thrust fault is estimated to be 381 km and excludes the two crosscutting subsidiary faults.

[14] Values of maximum displacement and fault length for the lobate scarps studied fall over two orders of magnitude (Figure 7). The values of γ of the population of thrust faults were obtained by a least squares fit to the D-L data with the intercept set to the origin [see *Cowie and Scholz*, 1992]. The γ of the lobate scarp thrust faults along the dichotomy boundary, using estimates of D based on $\theta = 25°$, is

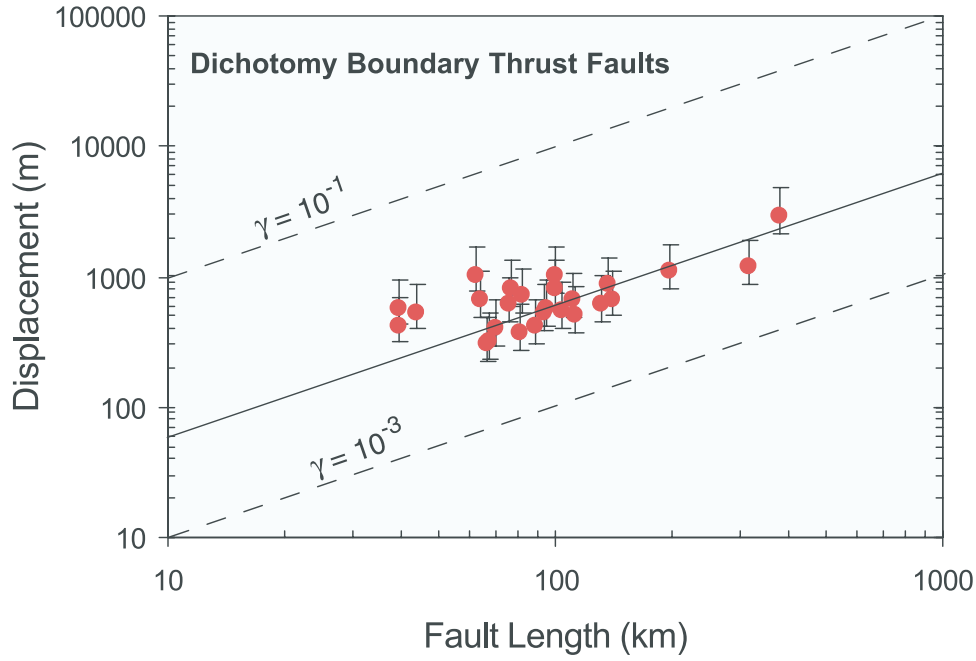

Figure 7. Log-log plot of maximum displacement as a function of fault length for 26 Martian lobate scarps. The ratio γ of the population of thrust faults were obtained by a linear fit to the *D-L* data with the intercept set to the origin [*Cowie and Scholz*, 1992]. $\gamma \cong 6.2 \times 10^{-3}$ using estimates of D based on fault plane dips $\theta = 25°$. The error bars indicate the range in displacement for fault plane dips of 15° to 35°.

$\sim 6.2 \times 10^{-3}$ ($n = 26$) (Tables 1 and 2) (Figure 7). This is in good agreement with previous estimates based largely on photoclinometrically derived topography [*Watters and Robinson*, 1999] and with estimates of the γ of mercurian lobate scarps ($\sim 6.5 \times 10^{-3}$) [*Watters et al.*, 2000]. There is almost an order of magnitude difference between the γ of terrestrial thrust fault populations ($\sim 8.0 \times 10^{-2}$) [*Watters et al.*, 2000] and thrust faults along the dichotomy boundary. The most likely explanation for the difference is the tectonic setting [*Watters et al.*, 2000]. Terrestrial thrust faults occur in foreland thrust belts located at convergent plate margins where the structures accumulate large amounts of strain and the deformation is driven by plate tectonics. The dichotomy boundary is probably more akin to a terrestrial passive margin [*Watters and Robinson*, 1999; *Watters*, 2003], and thrust faulting is more distributed.

3. Dichotomy Boundary

[15] One of the most compelling and enduring questions about geologic evolution of Mars is the origin of the hemispheric dichotomy. In the eastern hemisphere, the dichotomy boundary is marked by a relatively steep scarp and a dramatic elevation change. MOLA data indicate that the regional elevation change is greater than 2.5 km and up to 6 km in some areas [*Frey et al.*, 1998; *Smith et al.*, 1998, 1999, 2001; *Zuber et al.*, 2000]. In northern Arabia Terra, the dichotomy boundary has a maximum relief of $\sim$2.5 km (Figure 4). In the Amenthes-northern Terra Cimmeria region the boundary has a maximum relief of $\sim$3.5 km (Figure 1). In both regions the highlands at the dichotomy boundary generally slope toward the northern lowlands, however there are areas where this trend is reversed [see *Frey et al.*, 1998]. Thus, throughout much of the eastern hemisphere, the dichotomy boundary has a distinct topographic signature.

[16] The models proposed for the origin of the crustal dichotomy fall into two groups, one involving impact processes and the other involving internal processes. Impact models invoke either one giant impact [*Wilhelms and Squyres*, 1984; *McGill*, 1989] or multiple impacts [*Frey and Schultz*, 1988]. These models require that the dichotomy is very old (early or pre-Noachian), forming well before the end of the period of heavy bombardment. The impact origin is not strongly supported by MGS data [*Zuber*, 2001]. The lack of correlation of crustal thickness with the geological expression of the dichotomy, the noncircular outline of the northern lowlands, and the lack of other Utopia-scale circular zones of crustal thinning all argue against an impact origin [*Zuber et al.*, 2000; *Zuber*, 2001]. Models invoking internal processes involve thinning of the northern hemisphere crust by mantle convection [*Wise et al.*, 1979; *McGill and Dimitriou*, 1990; *Zhong and Zuber*, 2001; *Zuber*, 2001] or a period of plate tectonics [*Sleep*, 1994, 2000]. *McGill and Dimitriou* [1990] cite Late Noachian to Early Hesperian fracturing and faulting in the northern lowlands and along the dichotomy as evidence of a younger age of formation. They propose that the early northern crust was thinned and subsided through delamination or crustal erosion by mantle convection. The eroded crustal material is thought to have been globally dispersed [*McGill and Dimitriou*, 1990]. *Zhong and Zuber* [2001] invoke hemispheric-scale mantle convection with upwelling in one hemisphere and downwelling in the other. The predicted convection pattern results in preferential heating and crustal thinning in one hemisphere and crustal thickening in the other hemisphere [*Zhong and Zuber*, 2001; *Zuber*, 2001]. Mantle convection models predict extension [*McGill and Dimitriou*, 1990] and volcanism [*Zhong and Zuber*, 2001] in the northern lowlands that accompanied the formation of the crustal dichotomy, but do not explain the localized extensional and compressional deformation along the dichotomy boundary [*Watters and Robinson*, 1999; *Watters*, 2003].

[17] In the plate tectonic model proposed by *Sleep* [1994] the northern crust was removed by Late Noachian hemispheric subduction, the younger lowlands crust resulted from seafloor spreading, and the present dichotomy boundary marks relic plate margins. It is suggested that the boundary extending from the Tyrrhena region, through Amenthes and Terra Cimmeria, to Memnonia is a passive margin. Subduction of the proposed Boreal-Austral plate began in the Arabia region and extended through Tempe Terra to the northern part of the Tharsis Montes volcanic line, eventually extending as far south as Daedalla [*Sleep*, 1994]. Although the topography of the dichotomy boundary in Amenthes and Terra Cimmeria is consistent with that of terrestrial passive margins [*Frey et al.*, 1998], there is no evidence that the boundary in Arabia was an active subduction zone [*McGill*, 2000]. The general morphology of the dichotomy boundary (see below) and the tectonic features in northern Arabia Terra and in Amenthes-northern Terra Cimmeria, are very similar (Figures 1 and 4) [*Watters*, 2003].

[18] MGS magnetometer data indicate the presence of roughly parallel, linear magnetic features that alternate in polarity [*Connerney et al.*, 1999; *Acuna et al.*, 1999]. The most intense of magnetic sources occur in the southern highlands of Terra Cimmeria and Terra Sirenum, south of the dichotomy boundary [*Acuna et al.*, 1999]. One interpretation of the magnetic stripes is that they result from a process akin to seafloor spreading, formed during the early to mid Noachian when Mars had an active dynamo [*Connerney et al.*, 1999; *Acuna et al.*, 1999]. The lack of magnetic features in the northern lowlands suggests that the crustal dichotomy formed after the dynamo ceased to operate [*Acuna et al.*, 1999]. An altitude-normalized vertical component map of the crustal magnetic field indicates significant magnetic features are found in the northern lowlands [*Purucker et al.*, 2000]. If the dynamo did shut down early, these features may reflect thin cover over ancient magnetized crust [*Purucker et al.*, 2000].

[19] MOLA data have revealed a large number of subdued circular depressions in the northern lowlands, interpreted to be buried ancient impact basins [*Frey et al.*, 2002]. The cumulative size-frequency distribution of the quasi-circular depressions suggests that the number of craters beneath the northern plains is comparable to that exposed in the southern highlands. This suggests that the smooth and sparsely cratered northern plains are only a veneer on a surface as least as old as the southern highlands [*Frey et al.*, 2002]. However, MOLA data have also revealed evidence of buried basins in the highlands suggesting that the buried northern lowlands may be younger than the highlands [*Frey*,

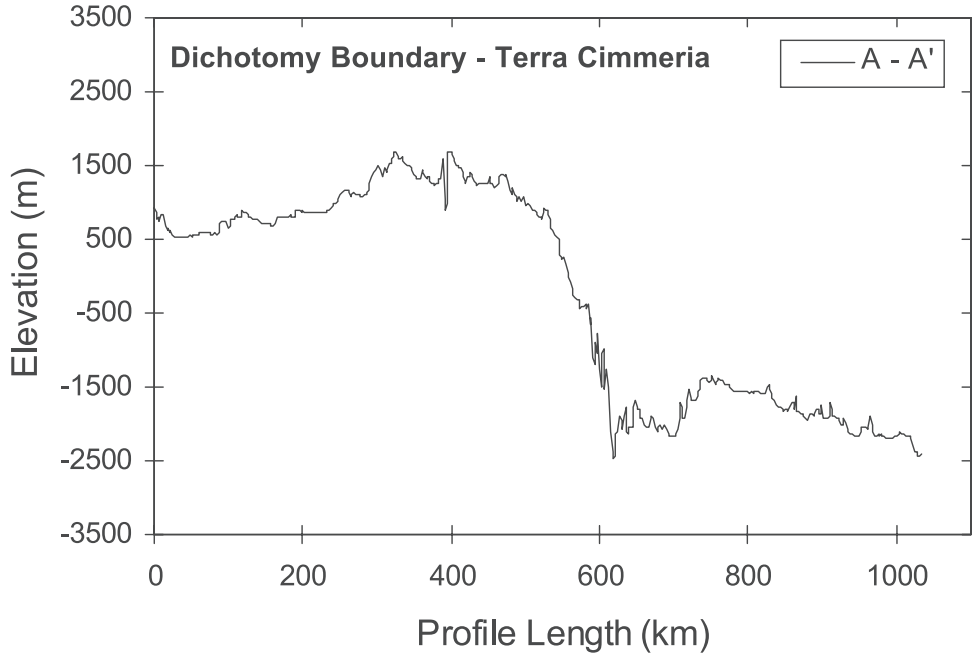

Figure 8. MOLA profile across the dichotomy boundary in northern Terra Cimmeria. Profile location is shown in Figure 1. Profile was derived from MOLA 1/32° per pixel resolution gridded data. Vertical exaggeration is ~100:1.

2002]. The age of the northern lowland crust and the timing of the resurfacing are major constraints on models for the origin of the crustal dichotomy [*Zuber*, 2001] and the evolution of the dichotomy boundary. If the dichotomy resulted from lithospheric recycling, evidence of buried impact basins in the northern lowlands indicates that it must have occurred in the Early Noachian.

[20] The tectonic features in the eastern hemisphere suggest a deformational event involving both extension and compression was connected with the formation of the dichotomy boundary [*Watters and Robinson*, 1999; *Watters*, 1993, 2003]. Thrust faulting of the highlands near the boundary appears to have occurred during the Late Noachian to Early Hesperian [*Maxwell and McGill*, 1988; *Wilhelms and Baldwin*, 1989; *Watters and Robinson*, 1999]. In the highlands of Amenthes-northern Terra Cimmeria and northern Arabia Terra, most lobate scarps are found between approximately 100 to 500 km from the dichotomy boundary (Figures 1 and 4) [*Watters*, 2003]. In northern Arabia Terra, another group of lobate are found from about 700 km to 1000 km from the boundary (Figure 4). These lobate scarps have orientations similar to other compressional tectonic features in Arabia Terra [see *Watters*, 1993]. The deformation along the dichotomy boundary suggests that it formed in the Late Noachian to Early Hesperian [*McGill and Dimitriou*, 1990; *Watters and Robinson*, 1999; *Watters*, 2003].

[21] Although the morphology of the dichotomy boundary in the eastern hemisphere varies, there are common elements, particularly in northern Terra Cimmeria and northern Arabia Terra. Along much of its length the dichotomy is characterized by a scarp and rise morphology [*Watters*, 2003]. This morphology is best preserved in northern Terra Cimmeria (Figure 8). Here the boundary is marked by a scarp where the slope reaches a maximum. The scarp transitions into a broad rise in the highlands, several hundred kilometers wide (Figure 8). The highlands beyond the rise, referred to as the back rise, are gently sloping. The extensional features are generally located on and adjacent to the slopes of the scarp and extend into the northern plains. The thrust faults, expressed by the lobate scarps, are usually located on the rise, although some may be found on the back rise. This is also the case for the thrust faults in northern Arabia Terra. Like northern Terra Cimmeria, the morphology of the boundary in northern Arabia Terra is marked by a scarp, a broad rise, and a gentle sloping back rise (Figure 9). Fractures and normal faults are found along and adjacent to the boundary scarp and thrust faults occur on the rise and back rise.

4. Discussion and Conclusions

[22] The morphology of the dichotomy boundary, the spatial relationship of tectonic features, and the time of their formation suggest that lithospheric flexure may have played a role in its formation [*Watters*, 2003]. The morphology of the dichotomy boundary, particularly in northern Terra Cimmeria, is very similar to profiles across terrestrial lithosphere that has been flexed by vertical loading [*Caldwell et al.*, 1976; *Turcotte*, 1979; *Turcotte and Schubert*, 1982]. The topography of the dichotomy boundary in northern Terra Cimmeria can be modeled by a semi-infinite or cracked lithosphere under a vertical load. The best-fit universal lithospheric deflection profile corresponds to an elastic thickness T_e of ~31 to 36 km [*Watters*, 2003]. This suggests the dichotomy boundary is the result of flexure of the southern highland lithosphere in response to vertical loading [*Watters*, 2003].

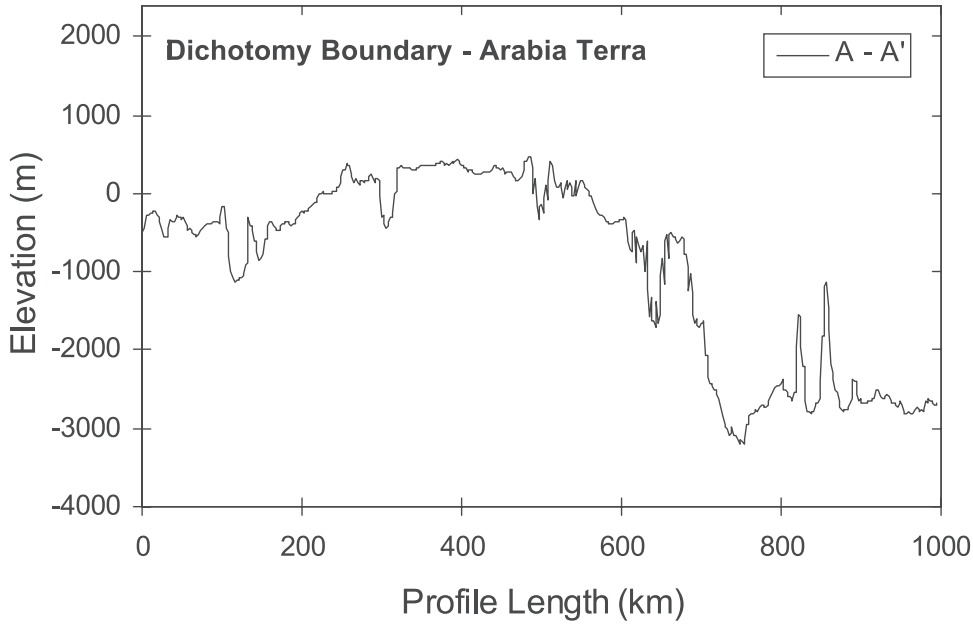

Figure 9. MOLA profile across the dichotomy boundary in northern Arabia Terra. Profile location is shown in Figure 4. Profile was derived from MOLA 1/32° per pixel resolution gridded data. Vertical exaggeration is ~100:1.

[23] There are several possible sources of the vertical load: 1) accumulation of volcanic and sedimentary material in the northern lowlands during the Late Noachian and Early Hesperian, 2) subsidence of the northern lowlands by convection driven crustal thinning, and 3) thermal contraction of initially hot lowland lithosphere. There is evidence from MOLA data of buried ridged plains material throughout the northern lowlands [*Zuber*, 2001; *Head et al.*, 2002]. The ridged plains, so named for the presences of wrinkle ridges that reflect folding and thrust faulting, appear to be Early Hesperian in age and are contiguous with exposed Early Hesperian-aged ridged plains [*Head et al.*, 2002]. The thickness of the ridged plains volcanics in the northern lowlands is estimated to be up to several kilometers [*Head et al.*, 2002]. Recent MGS-based gravity models indicate linear positive free-air anomalies in the lowlands along the dichotomy boundary [*Zuber et al.*, 2000; *Yuan et al.*, 2001]. These anomalies may represent the presence of thick accumulations of volcanic material in the northern lowlands along the margin of the southern highlands. Crustal thinning involves the removal and replacement of northern lowlands crust by mantle material [*McGill and Dimitriou*, 1990; *Zhong and Zuber*, 2001; *Zuber*, 2001], resulting in subsidence and a significant vertical load. If crustal thinning formed the dichotomy during the Late Noachian-Early Hesperian [*McGill and Dimitriou*, 1990], vertical loading may have been caused by a combination of subsidence and volcanic loading [*Watters*, 2003]. Vertical loading at terrestrial passive margins results from subsidence of cooling oceanic lithosphere [*Turcotte et al.*, 1977; *Turcotte*, 1979]. If the crustal dichotomy formed by plate recycling and the dichotomy boundary is analogous to a passive margin [*Sleep*, 1994], cooling and subsidence of northern lowlands lithosphere would have resulted in vertical loading. However, if plate recycling occurred it was very early and the ancient passive margin and the effects of loading due to cooling lithosphere would not likely be preserved in the present dichotomy boundary [*Watters*, 2003].

[24] Extensional and compressional bending stresses are generated by lithospheric flexure [*Turcotte*, 1979; *Turcotte et al.*, 1978; *Turcotte and Schubert*, 1982]. At the top of the lithosphere, the bending stresses are dominantly extensional, and the maximum occurs along the dichotomy boundary and in the adjacent lowlands [*Watters*, 2003]. Compressional surface bending stresses reach a maximum in the highlands at a distance of ~500 km from the dichotomy boundary, however, their magnitude is relatively low. Although at the base of the elastic lithosphere the bending stresses are compressional, it is unlikely that the magnitude was great enough to initiate faulting. Thus fracturing and normal faulting are predicted along the dichotomy boundary, but bending stresses do not account for the lobate scarps in the adjacent highlands [*Watters*, 2003].

[25] Thinning of northern lowlands crust by mantle convection will result in lithospheric stresses. The response of the elastic lithosphere to sub-crustal erosion is analogous to that of surface erosion where extensional stresses are generated in the area of erosion and compressional stresses are generated in the adjacent lithosphere [*Stein et al.*, 1979; *Zoback and Zoback*, 1980]. However, because in sub-crustal erosion crust is replaced by mantle, compressional stresses occur where crust is removed and extensional stresses occur in the adjacent lithosphere. This is inconsistent with the observed tectonic features along the dichotomy boundary. Stresses resulting from crustal thinning are significant. For a semi-infinite load, the fiber stress is given by

$$\sigma_{xx} = \frac{Eh\rho_r z}{\alpha^2(\rho_m - \rho_c)} \sin\left(\frac{x}{\alpha}\right) \exp\left(-\frac{|x|}{\alpha}\right) \quad (1)$$

where z is the vertical distance in the lithosphere relative to the neutral surface defined as positive up, ρ_c is the density of the crust, ρ_m is the density of the mantle, α is the flexural parameter, and h is the depth of the material removed [*Stein et al.*, 1979]. For $\alpha \cong 153$ km (based on the best-fit universal lithospheric deflection curve [*Watters*, 2003]), $T_e = 34$ km, $\rho_c = 2900$ kg m^{-3}, $\rho_m = 3400$ kg m^{-3}, the removal of 5 km of lowlands crust results in maximum surface stresses >600 MPa at $x = \pm 120$ km. These stresses are sufficient to cause thrust faulting in the lowlands along the dichotomy boundary and normal faulting of the highland rise. Although wrinkle ridges occur in the northern lowlands near the dichotomy boundary, their orientations are perpendicular rather than parallel to the dichotomy boundary [see *Head et al.*, 2002]. Thus flexure of the southern highlands by volcanic loading or crustal thinning of the northern lowlands cannot account for the observed thrust faults. Other sources of compressional stresses must be sought.

[26] Erosion of highland material along the dichotomy boundary is a possible source of compressional stress. It is estimated that the maximum compressional stress in the highlands due to erosion along the dichotomy boundary, approximated by a rectangular finite-width load 3 km high and 200 km wide, is ~140 MPa [*Watters*, 2003]. However, because the amount of post-flexure erosion of the highlands was not large enough to erase the topographic expression of flexure, this estimate is probably an upper limit. Although compressional stresses from flexure and erosion of the highlands along the dichotomy boundary may not have been large enough by themselves to initiate thrust faulting, they may have been superposed on compressional stresses due to global contraction. It has been shown that compressional deformation on Mars peaked during the Early Hesperian [*Watters*, 1993], corresponding to a peak in volcanic resurfacing [*Greeley and Schneid*, 1991; *Head et al.*, 2002]. This is reflected by the global-scale deformation of ridged plains, including those in the northern lowlands [*Head et al.*, 2002]. Compressional stresses due to global contraction are horizontally isotropic, and the resulting tectonic features will be expected to have no preferred orientation [see *Watters*, 1993]. The formation of lobate scarps in intercrater plains with no preferred orientation (i.e., Noachis Terra) [*Watters*, 1993] suggests that horizontally isotropic stresses in the eastern hemisphere during the Late Noachian-Early Hesperian were sufficient to cause thrust faulting. Thus compressional stresses from bending and erosion of the highlands only need to be large enough to cause a sufficient difference between the horizontal components to account for the orientations of thrust faults along the dichotomy boundary.

[27] In conclusion, the lobate scarps along the dichotomy boundary in the eastern hemisphere reflect thrust faulting of the southern highlands. Displacement on the thrust faults is generally about 1 km or less (see Tables 1 and 2) except in the case of the Amenthes Rupes thrust fault, where the displacement is on the order of 3 km. The *D-L* relationship of the lobate scarps is consistent with terrestrial and other planetary thrust fault populations. Thrust faulting is roughly coincident with Late Noachian to Early Hesperian fracturing and normal faulting along the dichotomy boundary. Thus extensional and compressional deformation were involved in the formation of the present-day dichotomy boundary. The long wavelength topography of the dichotomy boundary suggests it may have been formed by flexure of the southern highlands lithosphere. Although bending stresses due to flexure alone cannot explain the lobate scarps, thrust faulting of the highlands along the dichotomy boundary may have resulted from a combination of bending stresses, stresses due to erosion, and global contraction.

[28] **Acknowledgments.** I thank Francis Nimmo for his review and helpful discussions that greatly improved the manuscript, and Norman H. Sleep for helpful discussions. This research was supported by a grant from National Aeronautics and Space Administration's Mars Data Analysis Program.

References

Acuna, M. H., et al., Global distribution of crustal magnetization discovered by the Mars Global Surveyor MAG/ER Experiment, *Science*, *284*, 790–793, 1999.

Binder, A. B., Post-Imbrian global lunar tectonism: Evidence for an initially totally molten Moon, *Earth Moon Planets*, *26*, 117–133, 1982.

Binder, A. B., and H.-C. Gunga, Young thrust-fault scarps in the highlands: Evidence for an initially totally molten Moon, *Icarus*, *63*, 421–441, 1985.

Brewer, J. A., S. B. Smithson, J. E. Oliver, S. Kaufman, and L. D. Brown, The Laramide orogeny: Evidence from COCORP deep crustal seismic profiles in the Wind River mountains, Wyoming, *Tectonophysics*, *62*, 165–189, 1980.

Byerlee, J., Friction of rocks, *Pure Appl. Geophys.*, *116*, 615–626, 1978.

Caldwell, J. G., W. F. Haxby, D. E. Karig, and D. L. Turcotte, On the applicability of a universal elastic trench profile, *Earth. Planet. Sci. Lett.*, *31*, 239–246, 1976.

Cartwright, J. A., B. D. Trudgill, and C. S. Mansfield, Fault growth by segment linkage: An explanation for scatter in maximum displacement and trace length data from the Canyonlands Grabens of SE Utah, *J. Struct. Geol.*, *17*, 1319–1326, 1995.

Clark, R., and S. Cox, A modern regression approach to determining fault displacement-length scaling relationships, *J. Struct. Geol.*, *18*, 147–154, 1996.

Connerney, J. E., M. H. Acuna, P. J. Wasilewski, N. F. Ness, H. Reme, C. Mazelle, D. Vignes, R. P. Lin, D. L. Mitchell, and P. A. Cloutier, Magnetic lineations in the ancient crust of Mars, *Science*, *284*, 794–798, 1999.

Cordell, B. M., and R. G. Strom, Global tectonics of Mercury and the Moon, *Phys. Earth Planet. Inter.*, *15*, 146–155, 1977.

Cowie, P. A., and C. H. Scholz, Displacement-length scaling relationship for faults: Data synthesis and discussion, *J. Struct. Geol.*, *14*, 1149–1156, 1992.

Dawers, N. H., and M. H. Anders, Displacement-length scaling and fault linkage, *J. Struct. Geol.*, *17*, 607–614, 1995.

Frey, H., Large buried and visible basins on Mars: Total population ages of the highlands and lowlands (abstract), *Geol. Soc.*, 26-3, 2002.

Frey, H., and R. A. Schultz, Large impact basins and the mega-impact origin for the crustal dichotomy on Mars, *Geophys. Res. Lett.*, *15*, 229–232, 1988.

Frey, H., S. E. Sakimoto, and J. H. Roark, The MOLA topographic signature at the crustal dichotomy boundary zone on Mars, *Geophys. Res. Lett.*, *25*, 4409–4412, 1998.

Frey, H., S. E. Sakimoto, and J. H. Roark, Discovery of a 450 km diameter, multi-ring basin on Mars through analysis of MOLA topographic data, *Geophys. Res. Lett.*, *26*, 1657–1660, 1999.

Frey, H. V., J. H. Roark, K. M. Shockey, E. L. Frey, and S. E. H. Sakimoto, Ancient lowlands on Mars, *Geophys. Res. Lett.*, *29*(10), 1384, doi:10.1029/2001GL013832, 2002.

Greeley, R., and J. E. Guest, Geologic map of the eastern equatorial region of Mars, scale 1:15,000,000, *U.S. Geol. Surv. Misc. Invest. Ser. Map*, *I-1802-B*, 1987.

Greeley, R., and B. D. Schneid, Magma generation on Mars: Amounts, rates and comparisons with Earth, Moon, and Venus, *Science*, *254*, 996–998, 1991.

Gries, R., Oil and gas prospecting beneath Precambrian of foreland thrust plates in Rocky Mountains, *Am. Assoc. Pet. Geol. Bull.*, *67*, 1–28, 1983.

Head, J. W., III, M. A. Kreslavsky, and S. Pratt, Northern lowlands of Mars: Evidence for widespread volcanic flooding and tectonic deformation in the Hesperian Period, *J. Geophys. Res.*, *107*(E1), 5003, doi:10.1029/2000JE001445, 2002.

Howard, K. A., and W. R. Muehlberger, Lunar thrust faults in the Taurus-Littrow region, Apollo 17 Preliminary Science Report, *NASA Spec. Publ., NASA SP-330*, 31-32–31-25, 1973.

Jaeger, J. C., and N. G. W. Cook, *Fundamentals of Rock Mechanics*, 3rd ed., 593 pp., Chapman and Hall, New York, 1979.

Lucchitta, B. K., Mare ridges and related highland scarps—Results of vertical tectonism, *Geochim. Cosmochim. Acta*, *3*, suppl., 2761–2782, 1976.

Maxwell, T. A., and G. E. McGill, Ages of fracturing and resurfacing in the Amenthes Region, Mars, *Proc. Lunar Planet. Sci. Conf. 18th*, 701–711, 1988.

McGill, G. E., Buried topography of Utopia, Mars: Persistence of a giant impact depression, *J. Geophys. Res.*, *94*, 2753–2759, 1989.

McGill, G. E., Crustal history of north central Arabia Terra, Mars, *J. Geophys. Res.*, *105*, 6945–6960, 2000.

McGill, G. E., and A. M. Dimitriou, Origin of the Martian global dichotomy by crustal thinning in the late Noachian or early Hesperian, *J. Geophys. Res.*, *95*, 12,595–12,605, 1990.

Melosh, H. J., and W. B. McKinnon, The tectonics of Mercury, in *Mercury*, edited by F. Vilas, C. R. Chapman, and M. S. Matthews, pp. 374–400, Univ. of Ariz. Press, Tucson, 1988.

Neumann, G. A., D. D. Rowlands, F. G. Lemoine, D. E. Smith, and M. T. Zuber, Crossover analysis of Mars Orbiter Laser Altimeter data, *J. Geophys. Res.*, *106*, 23,753–23,768, 2001.

Phillips, R. J., et al., Ancient geodynamics and global-scale hydrology on Mars, *Science*, *291*, 2587–2591, 2001.

Purucker, M., D. Ravat, H. Frey, C. Voorhies, T. Sabaka, and M. Acuna, An altitude-normalized magnetic map of Mars and its interpretation, *Geophys. Res. Lett.*, *27*, 2449–2452, 2000.

Schultz, R. A., Displacement-length scaling for terrestrial and Martian faults: Implications for Valles Marineris and shallow planetary grabens, *J. Geophys. Res.*, *102*, 12,009–12,015, 1997.

Schultz, R. A., Understanding the process of faulting: Selected challenges and opportunities at the edge of the 21st century, *J. Struct. Geol.*, *21*, 985–993, 1999.

Schultz, R. A., and A. N. Fori, Fault-length statistics and implications of graben sets at Candor Mensa, Mars, *J. Struct. Geol.*, *18*, 272–383, 1996.

Schultz, R. A., and T. R. Watters, Forward mechanical modeling of the Amenthes Rupes thrust fault on Mars, *Geophys. Res. Lett.*, *28*, 4659–4662, 2001.

Sleep, N. H., Martian plate tectonics, *J. Geophys. Res.*, *99*, 5639–5656, 1994.

Sleep, N. H., Evolution of the mode of convection within terrestrial planets, *J. Geophys. Res.*, *105*, 17,563–17,578, 2000.

Smith, D. E., et al., Topography of the Northern Hemisphere of Mars from the Mars Orbiter Laser Altimeter, *Science*, *279*, 1686–1692, 1998.

Smith, D. E., et al., The global topography of Mars and implications for surface evolution, *Science*, *279*, 1495–1503, 1999.

Smith, D. E., et al., Mars Orbiter Laser Altimeter: Experiment summary after the first year of global mapping of Mars, *J. Geophys. Res.*, *106*, 23,689–23,722, 2001.

Stein, S., N. H. Sleep, R. J. Geller, S.-C. Wang, and G. C. Kroeger, Earthquakes along the passive margin of eastern Canada, *Geophys. Res. Lett.*, *6*, 537–540, 1979.

Stone, D. S., Geologic interpretation of seismic profiles, Big Horn Basin, Wyoming, Part I: East Flank, in *Seismic Exploration of the Rocky Mountain Region*, edited by R. R. Gries and R. C. Dyer, pp. 165–174, Rocky Mt. Assoc. of Geol., Denver, Colo., 1985.

Strom, R. G., N. J. Trask, and J. E. Guest, Tectonism and volcanism on Mercury, *J. Geophys. Res.*, *80*, 2478–2507, 1975.

Turcotte, D. L., Flexure, *Adv. Geophys*, *21*, 51–86, 1979.

Turcotte, D. L., and G. Schubert, *Geodynamics*: *Application of Continuum Physics to Geological Problems*, 450 pp., John Wiley, New York, 1982.

Turcotte, D. L., J. L. Ahern, and J. M. Bird, The state of stress at continental margins, *Tectonophysics*, *42*, 1–28, 1977.

Turcotte, D. L., D. C. McAdoo, and J. G. Caldwell, An elastic-perfectly plastic analysis of the bending of the lithosphere at a trench, *Tectonophysics*, *47*, 193–205, 1978.

Walsh, J., and J. Watterson, Analysis of the relationship between displacements and dimensions of faults, *J. Struct. Geol.*, *10*, 239–247, 1988.

Watters, T. R., Wrinkle ridge assemblages on the terrestrial planets, *J. Geophys. Res.*, *93*, 10,236–10,254, 1988.

Watters, T. R., Compressional tectonism on Mars, *J. Geophys. Res.*, *98*, 17,049–17,060, 1993.

Watters, T. R., Lithospheric flexure and the origin of the dichotomy boundary on Mars, *Geology*, *31*, 271–274, 2003.

Watters, T. R., and M. S. Robinson, Lobate scarps and the origin of the Martian crustal dichotomy, *J. Geophys. Res*, *104*, 18,981–18,990, 1999.

Watters, T. R., and R. A. Schultz, Fault geometry of planetary lobate scarps: Listric verses Planar (abstract), *Proc. Lunar Planet. Sci. Conf. 33rd*, 1668–1669, 2002.

Watters, T. R., M. S. Robinson, and A. C. Cook, Topography of lobate scarps on Mercury: New constraints on the planet's contraction, *Geology*, *26*, 991–994, 1998.

Watters, T. R., R. A. Schultz, and M. S. Robinson, Displacement-length relations of thrust faults associated with lobate scarps on mercury and Mars: Comparison with terrestrial faults, *Geophys. Res. Lett.*, *27*, 3659–3662, 2000.

Watters, T. R., M. S. Robinson, and A. C. Cook, Large-scale lobate scarps in the southern hemisphere of Mercury, *Planet. Space Sci.*, *49*, 1523–1530, 2001.

Watters, T. R., R. A. Schultz, M. S. Robinson, and A. C. Cook, The mechanical and thermal structure of Mercury's early lithosphere, *Geophys. Res. Lett.*, *29*(11), 1542, doi:10.1029/2001GL014308, 2002.

Wilhelms, D. E., and R. J. Baldwin, The role of igneous sills in shaping the Martian uplands, *Lunar Planet Sci.*, *XIX*, 355–365, 1989.

Wilhelms, D. E., and S. W. Squyres, The Martian hemispheric dichotomy may be due to a giant impact, *Nature*, *309*, 138–140, 1984.

Wise, D. U., M. P. Golombek, and G. E. McGill, Tharsis province of Mars: Geologic sequence, geometry and a deformation mechanism, *Icarus*, *38*, 456–472, 1979.

Wojtal, S. F., Changes in fault displacement populations correlated to linkage between faults, *J. Struct. Geol.*, *18*, 265–279, 1996.

Yuan, D.-N., W. L. Sjogren, A. S. Konopliv, and A. B. Kucinskas, Gravity field of Mars: A 75th degree and order model, *J. Geophys. Res.*, *106*, 23,377–23,401, 2001.

Zhong, S., and M. T. Zuber, Degree-1 mantle convection and the crustal dichotomy on Mars, *Earth. Planet. Sci. Lett.*, *189*, 75–84, 2001.

Zoback, M. L., and M. Zoback, State of stress in the conterminous United States, *J. Geophys. Res.*, *85*, 6113–6156, 1980.

Zuber, M. T., The crust and mantle of Mars, *Nature*, *412*, 220–227, 2001.

Zuber, M. T., D. E. Smith, S. C. Solomon, D. O. Muhleman, J. W. Head, J. B. Garvin, J. B. Abshire, and J. L. Bufton, The Mars Observer Laser Altimeter investigation, *J. Geophys. Res.*, *97*, 7781–7797, 1992.

Zuber, M. T., et al., Internal structure and early thermal evolution of Mars from Mars Global Surveyor topography and gravity, *Science*, *287*, 1788–1793, 2000.

T. R. Watters, Center for Earth and Planetary Studies, National Air and Space Museum, Smithsonian Institution, Washington, DC 20560-0315, USA. (twatters@nasm.si.edu)